

An Extension to the Projected Range
Algorithm (PRAL) to give Energy
Deposition Profiles

R.P.Webb and I.H.Wilson
Department of Electronic and
Electrical Engineering,
University of Surrey,
Guildford, Surrey, GU2 5XH.

ABSTRACT.

The PRAL programme for energetic ion ranges already gives the most accurate prediction of the first two moments of ion implantation profiles. Yet this algorithm is based upon a very simple formulism and is very fast to compute. We have extended this algorithm to give energy deposition profiles. These can be used to give estimates of ion created disorder. Comparisons with the Monte Carlo programme TRIM show these results to be of good accuracy. The advantage of this algorithm over the Monte Carlo programme is in the speed of execution. The energy deposition profile is obtained in times slightly longer than that for range profiles.

Disorder profiles are becoming more and more sought after, particularly in device fabrication areas as implantation in single crystals is becoming extensively used. The implant can often relocate in the implantation induced damage distribution during annealing. This algorithm gives a fast technique for predicting these profiles.

Introduction.

The Projected Range Algorithm (PRAL) is an implantation range profile algorithm obtained by J.P.Biersack [1] based upon a diffusional model of the slowing down of an ion. This algorithm was later verified by Biersack [2] to be consistent with Boltzmann Transport theory. The Biersack formulism has the advantage over other algorithms [3-8] in that it is fast and flexible. The speed of

execution derives from the fact that to obtain the first two moments of the implantation distribution one need only solve a set of three first order differential equations. These can be solved easily numerically and in such a way that they yield values for all ion energies upto the point of interest. The algorithm is flexible in that as it is a numerical solution it can employ any formulation of stopping power available - this is usually split into two parts (nuclear S_n and electronic S_e) and the Biersack algorithm can also include nuclear and electronic straggle. Currently PRAL uses the Biersack and Ziegler universal stopping powers [9]. These are based upon a fit to a set of Hartree-Fock-Slater calculations these have been compared to available experimental potential data and it has been found that this form of universal stopping is the most accurate of the universal type functions to date [10].

The determination of the spatial distribution of radiation damage is of particular interest to workers using ion irradiation to produce an amorphous region in the surface of single crystals so that subsequent implantation will avoid channelling effects. Before an estimate of the dose and energy of this preamorphisation irradiation can be made, however, simple estimates of the damage profile are needed. Adequate approximations to find energy deposition profiles from ion implantation range profiles have been described by Gibbons [11] and Fritzsche [12]. In both of these previous treatments, severe approximations were made as to the shape of the ion energy distribution [11] or the stopping power [12]. These approximations give rise to inaccuracies and to the creation of a low energy limit of validity for the procedures. It is the purpose of the following to describe the method currently used by the PRAL.ED algorithm to obtain energy deposition profiles from projected range data. The procedure is such that it allows calculation even at quite low energies and fewer approximations are enforced.

Energy Deposition Distributions.

To obtain a damage distribution, we must calculate the fraction of the initial ion energy, which is ultimately transferred to the solid by elastic (nuclear) collisions. The energy transfer (but not the energy transport) of the recoils can be included to allow for the reduction in overall

nuclear energy deposition due to electronic energy loss of the recoils themselves. There have been some studies of the effect of ignoring the recoil transport and these effects can be significant in some cases [13,14]. Work is currently under way to include the effects of recoil transport utilising a second stage PRAL calculation to determine the range of the recoils. For the purposes of the work presented here, we will assume this to be relatively minor.

The energy loss of the incident particle per unit path length, ds , is known (S_t) and this can be split into two separate terms S_n (nuclear energy loss) and S_e (electronic energy loss). The unknown is the energy loss per unit length, dx , perpendicular to the surface. This function of x will determine the damage distribution. The relation between these two energy loss functions has been given by Gibbons [11] as:

$$(dE/dx)_n' = \int_0^{E_0} P(E_0, E, x) * S_n(E) * ds/dx * dE \quad \dots \dots \dots (1)$$

where E_0 is the initial energy of the incident ion and P is the probability that the ion will have an energy E at depth x .

This gives the energy deposited by the ion in nuclear collisions to the recoils. To find out how much energy the recoils themselves actually deposit in nuclear collisions, we must multiply the distribution over energy by $v(E)$ - the fraction of energy which recoils transfer to the solid by elastic collisions. Thus equation 1 becomes:

$$(dE/dx)_n = \int_0^{E_0} P(E_0, E, x) * S_n(E) * ds/dx * v(E) * dE \quad \dots \dots (2)$$

Similarly it is possible to evaluate the inelastic energy loss (dE/dx) due to electronic collisions of both the recoils and the ion:

$$(dE/dx)_e = \int_0^{E_0} P(E_0, E, x) * S_e(E) * ds/dx * dE \quad \dots \dots \dots (3)$$

Clearly these two equations must satisfy the normalisation condition:

$$\int_0^{\infty} ((dE/dx)_n + (dE/dx)_e) dx = E_0 \dots\dots\dots (4)$$

Gibbons [11] method of solution was to approximate the function $P(E_0, E, x)$ by a rectangular distribution and to set $v(E)$ to a constant. The integral in equation 2 is then reduced to the integration of the stopping power. Gibbons [11] gives a graphical representation of this integral based upon Firsov [15] stopping for boron into silicon. For evaluation of this and other systems, this proves to be severely cumbersome as values must be determined from the graph. Fritzsche [12], on the other hand, assumed $P(E_0, E, x)$ to be a gaussian and approximated the energy loss function by the addition of two step functions. This yields a solution in terms of error functions which are readily available in tables. This method of solution has the disadvantage that, in order to model the energy loss function as two step functions, one can only consider cases above the nuclear stopping power maximum. This generally limits the calculation to fairly high energy. Also, the constraint on $P(E_0, E, x)$ to be gaussian is somewhat restrictive.

Here, we will follow along similar lines to Gibbons [11] in determining the energy distribution of the ions in the solid $P(E_0, E, x)$. We will assume that at depth $x=0$ (the surface) all ions enter with an initial energy E_0 . Further, when the ions have no energy ($E=0$), they will form the range profile as a function of x . Thus the energy distribution function $P(E_0, E, x)$ must spread from this initial monoenergetic state to the final range profile as shown in figure 1 (after Gibbons [11]) below.

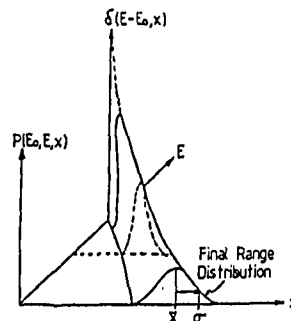


Figure 1.

After Gibbons. The variation of Energy Distribution Function with depth, x .

Similarly to Fritzsche [12], we will assume that the energy distribution function will be gaussian for fixed energy and two half gaussians for fixed depth (see figure 2 below). We will also assume that the standard deviations ($\sigma_r(E1,E0)$, $\sigma_1(x1,E0)$ and $\sigma_2(x1,E0)$) and the means ($E1(x1,E0)$, $R(E1,E0)$) of these distributions can given by the simple form:.

$$\begin{aligned}
 \sigma_r(E1,E0) &= \sigma(1-E1/E0) && \dots\dots \\
 \sigma_1(x1,E0) &= E0(x1.\sigma / ((\bar{x}-\sigma).\bar{x})) && \dots\dots | \\
 \sigma_2(x1,E0) &= E0(x1.\sigma / ((x+\sigma).\bar{x})) && \dots\dots | \dots\dots (5) \\
 R(E1,E0) &= \bar{x}(1-E1/E0) && \dots\dots | \\
 E1(x1,E0) &= E0(1-x1/\bar{x}) && \dots\dots |
 \end{aligned}$$

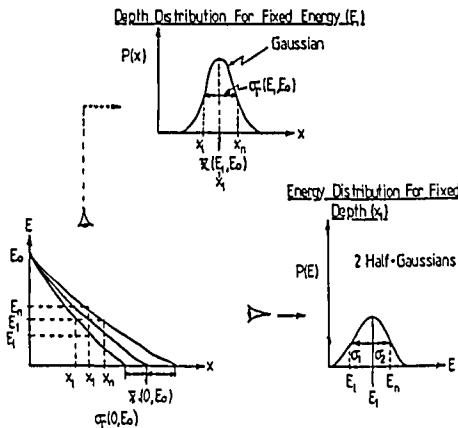
where \bar{x} and σ are the range and standard deviation of the ion range profile.

With these approximations, one can derive a general form for the energy distribution function $P(E0,E,x)$ as follows:

$$P(E0,E,x) = \frac{2\sigma_e}{2(\sigma_1 + \sigma_2)} \cdot \exp\left\{-\frac{[E-E1(x,E0)]^2}{2\sigma_e^2}\right\} \dots\dots (6)$$

$$\text{where } \sigma_e = \begin{cases} \sigma_1 & E < E1(x,E0) \\ \sigma_2 & E > E1(x,E0) \end{cases}$$

Figure 2. Energy Distributions Used In Calculations



Fritzsche [12] here took an average of σ and σ to enforce $P(E0,E,x)$ to gaussian form. Also in this earlier work $v(E).ds/dx$ was considered to be a constant. In this work we will assume that, for

most cases of interest, ds/dx will be constant with energy and thus be given by:

$$ds/dx = xt/\bar{x} \dots\dots\dots (7)$$

where xt is the total pathlength of the ion - this is easily evaluated as the integral of the stopping power - this is evaluated as routine in PRAL.

To evaluate the fraction of energy deposited in nuclear collisions, we use the method of Lindhard et al. [16] using a numerical approximation [17] to the universal function $g(\xi)$:

$$v(E) = 1/(1+k.g(\xi)) \dots\dots\dots (8)$$

$$g(\xi) = 3.4008 \xi^{1/6} + 0.40244 \xi^{3/4} + \xi$$

$$k = 0.1337.Z2^{1/6} (Z2/M2)^{1/2}$$

$$= E.a/(Z2.e)$$

$$a = (9 \pi^2 / (128.Z2))^{1/3} .a0/\sqrt{2}$$

where $a0$ is the Bohr radius, e is the electronic charge, $Z2$ and $M2$ are the atomic number and atomic mass of the recoiling particles.

The above equations can be combined and the resulting integrals solved numerically by dividing the energy distribution into a number of parts, treating the stopping power as constant at each division, thus expressing the integral of $P(E0,E,x1)$ over the energy division as an error function. This results in the following summations:

$$(dE/dx)_n = \frac{2xt.\sigma_e}{\bar{x}(\sigma_1 + \sigma_2)} \left\{ \operatorname{erf} \left(\frac{(E_{i+1}-E_1)}{\sqrt{2}\sigma_e} \right) - \operatorname{erf} \left(\frac{(E_i-E_1)}{\sqrt{2}\sigma_e} \right) \right\} .S_n(E_i) .v(E_i)$$

$$(dE/dx)_e = \frac{2xt.\sigma_e}{\bar{x}(\sigma_1 + \sigma_2)} \left\{ \operatorname{erf} \left(\frac{(E_{i+1}-E_1)}{\sqrt{2}\sigma_e} \right) - \operatorname{erf} \left(\frac{(E_i-E_1)}{\sqrt{2}\sigma_e} \right) \right\} .S_e(E_i)$$

These equations, together with equation 4, can now be used to determine both electronic and nuclear energy deposition profiles. From the nuclear energy deposition profile, it is a simple matter to convert to displacement damage profile,

$N_d(x)$, by using the modified Kinchen-Peaslee formula [18]:

$$N_d = KD \cdot (dE/dx)_n / (2Ed) \dots\dots\dots (10)$$

where KD is the displacement efficiency of the order 0.8;
 Ed is the displacement energy of the order 10-50 eV.

Results and Comparisons.

We have chosen to compare the energy deposition profiles obtained by the method outlined above to those generated using the Monte Carlo code TRIM [19]. This code follows individual ion

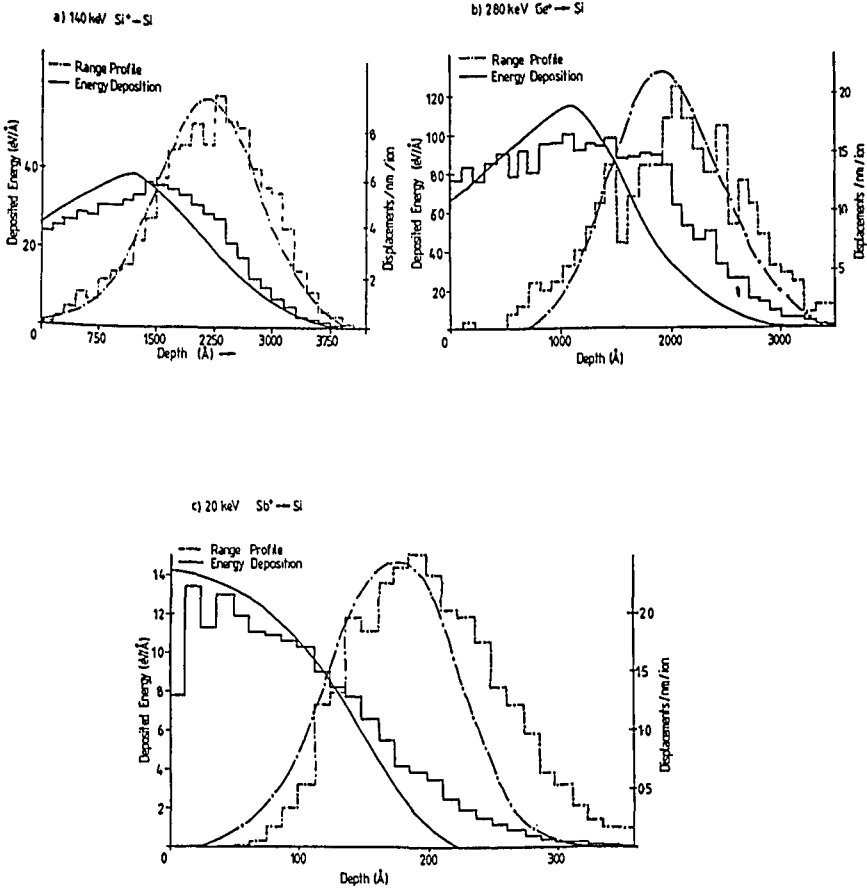


Figure 3. Comparison of TRIM (histograms) and PRAL.ED (smooth curves).

trajectories, allowing the particles to interact through a series of binary collisions. The stopping powers used in this programme are the same as those used in the PRAL code.

Shown over in figure 3 is a comparison of the energy deposition and range profiles as predicted by TRIM and using the procedure outlined above - PRAL.ED. Three comparisons have been made.

Figure 3 shows that there is good agreement between PRAL.ED and TRIM, even in the case of the low energy irradiation. This would not have been possible using either the Gibbons [11] approach or the Fritzsche [12] technique. Also included on figure 3 is a displacements/nm per ion scale. This has been calculated from equation 10.

In conclusion, it has been demonstrated that this technique can produce realistic energy deposition functions. The primary advantage is that this code is fast - typically, 2 orders of magnitude faster than the Monte Carlo technique (assuming 1000 individual ion trajectories).

Work is currently in hand to extend this code to allow layered structures and to include recoil motion.

References

- 1) Biersack, J.P.: Nucl. Instrum. Methods, 182/183, 199, (1981).
- 2) Biersack, J.P.: Z. Phys. A - Atoms and Nuclei, 305, 95, (1982).
- 3) Lindhard, J., Scharff, M., Schiott, H.E.: Mat. Fys. Medd. Dan. Vid. Selsk., 33, 14, (1963).
- 4) Brice, D.K.: in "Ion Implantation", Eds. F.H. Eisen and L.T.Chadderton (Gordon and Breach, London 1971) p.101.
- 5) Winterbon, K.B., Sigmund, P. and Saunders, J.B.: Mat. Fys. Medd. Dan. Vid Selsk., 37(14), (1970).
- 6) Winterbon, K.B.: "Ion Implantation Range and Energy Deposition Distributions" (IFI/Plenum Data Company, 1975).
- 7) Gibbons, J.F., Johnson, W.S. and Mylroie, S.W.: "Projected Range Statistics", 2nd Ed. (1975) dist. Halstead Press.
- 8) Ashworth, D.G., Moulavi-Kakhki, M. and Anand, K.V.: J. Phys. C - Solid State Phys., 17, 2449, (1984).
- 9) Biersack, J.P. and Ziegler, J.F.: Nucl. Instrum. Methods, 194, 93, (1982)
- 10) O'Conner, J.T. and Biersack, J.P.:

(Unpublished).

- 11) Gibbons, J.F.: Proc. IEEE 60(6), 1062, (1972).
- 12) Fritzsche, C.R.: Appl. Phys., 12, 347, (1977).
- 13) Gibson, J.B., Goland, A.N., Milgram, M. and Vineyard, G.H. Phys. Rev., 120, 1229, (1960).
- 14) Harrison Jr., D.E. and Webb, R.P.: Nucl. Instrum. Methods, 218, 727, (1983).
- 15) Firsov, O.B.: Zh. Eksp. Teor. Fiz., 36, 1517, (1959). (Sov. Phys. JETP 36, 1076, (1959)).
- 16) Lindhard, J., Nielson, V., Scharff, M. and Thomsen, P.V.: Kgl. Dan. Vidensk. Jelsk. Mat.-fys. Medd., 33(10), (1963).
- 17) Robinson, M.T.: in "Nuclear Fusion Reactors", British Nuclear Energy Society, London, 364, (1970).
- 18) Torrens, I.M. and Robinson, M.T.: in "Radiation Induced Voids in Metals", Eds. J.W. Corbett and L.C. Ianniello, USAEC Report, CONF-710601, 739, (1972).
- 19) Biersack, J.P. and Haggmark, L.G.: Nucl. Instrum. Methods, 174, 257, (1980).